Journal of Biotechnology 308 (2020) 63–73

Contents lists available at ScienceDirect

Journal of Biotechnology

journal homepage: www.elsevier.com/locate/jbiotec

Tracking Yeast Metabolism and the Crabtree Effect in Real Time via CO_2 Production using Broadband Acoustic Resonance Dissolution Spectroscopy (BARDS)

M. Rizwan Ahmed[a], Nicholas Doyle[a], Cathal Connolly[b], Seán McSweeney[d], Jacob Krüse[e], John Morrissey[c], Michael B. Prentice[c], Dara Fitzpatrick[a,*]

[a] School of Chemistry, Analytical and Biological Chemistry Research Facility (ABCRF), University College Cork, Ireland
[b] Alltech, Sarney, Dunboyne, County Meath, Ireland
[c] School of Microbiology, University College Cork, Ireland
[d] BARDS Acoustic Science Labs (BASL), Cork, Ireland
[e] Kinetox, Beilen, the Netherlands

ARTICLE INFO

Keywords:
Yeast
Spectroscopy
Acoustics
Crabtree effect
Metabolism
Viability and vitality

ABSTRACT

In this study, a new approach to measure metabolic activity of yeast via the Crabtree effect is described. BARDS is an analytical technique developed to aid powder and tablet characterisation by monitoring changes in the compressibility of a solvent during solute dissolution. It is a rapid and simple method which utilises a magnetic stir bar to mix added solute and induce the acoustic resonance of a vessel containing a fixed volume of solvent. In this study it is shown that initiation of fermentation in a yeast suspension, in aqueous buffer, is accompanied by reproducible changes in the frequency of induced acoustic resonance. These changes signify increased compressibility of the suspension due to CO_2 release by the yeast. A simple standardised BARDS protocol reveals yeast carbon source preferences and can generate quantitative kinetic data on carbon source metabolism which are characteristic of each yeast strain. The Crawford-Woods equation can be used to quantify total gaseous CO_2 produced by a given number of viable yeast when supplied with a fixed amount of carbon source. This allows for a value to be calculated for the amount of gaseous CO_2 produced by each yeast cell. The approach has the potential to transform the way in which yeast metabolism is tracked and potentially provide an orthogonal or surrogate method to determining viability, vitality and attenuation measurements in the future.

1. Introduction

Yeasts are unicellular fungi widespread in aerial, aquatic and terrestrial environments. The yeast *Saccharomyces cerevisiae* is one of the simplest eukaryotes and provided one of the first eukaryotic genome sequences (Fleet, 1998; Goffeau et al., 1996). It is a globular shaped organism with a size ranging between $5-10\,\mu m$ and is the most commonly found strain of yeast, widely known as baker's yeast or brewing yeast (Guilliermond, 1920). *S. cerevisiae* is one of the most extensively studied eukaryotes in biological research and is used in the production of biotechnology products globally and plays a pivotal role in the baking and brewing industries (Oliver et al., 1992; White, 1954). Therefore, monitoring the products of yeast metabolism is of significant importance.

Yeast metabolize sugars aerobically or anaerobically depending upon the environmental conditions. Yeast breaks down sugars into CO_2, water and energy in the form of adenosine triphosphate (ATP) under aerobic conditions. This involves the tricarboxylic acid (TCA) cycle and oxidative phosphorylation in mitochondria and the overall reaction involved during the process is given in Eq. (1) (Nilsson and Nielsen, 2016; Pfeiffer and Morley, 2014).

$$C_6H_{12}O_6 + 6O_2 \rightarrow 6CO_2 + 6H_2O + \text{energy} \quad (18\ ATP) \qquad (1)$$

In the general absence of oxygen, yeast metabolizes sugars and produces CO_2 and ethanol by fermentation. The fermentation reaction involves a series of chemical reactions and the action of various enzymes. The simplified overview of the metabolic process begins with the conversion of glucose ($C_6H_{12}O_6$) to pyruvic acid (CH_3-CO-COOH) by utilising the hydrogen carrier nicotinamide adenine dinucleotide (NAD) present in the yeast cell (Harden and Young, 1906).

* Corresponding author.
E-mail address: d.fitzpatrick@ucc.ie (D. Fitzpatrick).

https://doi.org/10.1016/j.jbiotec.2019.11.016
Received 23 August 2019; Received in revised form 20 November 2019; Accepted 27 November 2019
Available online 30 November 2019
0168-1656/

$$\text{Yeast} + C_6H_{12}O_6 + 2NAD^+ \rightarrow 2CH_3\text{-}CO\text{-}COOH + 2NADH + 2H^+ \quad (2)$$

The enzyme zymase converts the pyruvic acid to ethanol and carbon dioxide using NADH (Kresge et al., 2005).

$$CH_3 - CO - COOH + NADH + H^+ \rightarrow C_2H_5OH + CO_2 + NAD^+ \quad (3)$$

Overall yeast fermentation of sugars (represented by glucose) is described as:

$$C_6H_{12}O_6 \rightarrow 2C_2H_5OH + 2CO_2 + 2\ ATP \quad (4)$$

Eqs. (1) and (4) show that for a given amount of carbohydrate substrate, metabolism by respiration produces more CO_2 and ATP than metabolism by fermentation. Paradoxically, *S. cerevisiae* and some other yeast strains use relatively inefficient fermentation rather than respiration to metabolise glucose even in aerobic conditions when an excess of glucose is supplied (Pfeiffer and Morley, 2014). This phenomenon is known as the Crabtree effect and can be induced in yeast suspensions by supplying glucose above a concentration of ~0.32 % w/v. The Crabtree effect may represent a trade-off in cellular protein allocation during rapid growth where fermentation is favoured because it requires less enzyme mass per molecule of ATP generated than respiration (Nilsson and Nielsen, 2016). An additional factor affecting yeasts metabolic rate is a requirement for a variety of transporters for different monosaccharides and disaccharides to pass through the plasma membrane to the cytoplasm for metabolism (Lagunas, 1993).

Balloon inflation by CO_2 excretion from yeast suspensions metabolising glucose is a well-known popular science demonstration and CO_2 bubbles have been seen in the cytoplasm of glucose fermenting *Saccharomyces* strains (Swart et al., 2012). We therefore hypothesized that CO_2 bubble evolution by a yeast suspension in response to a sugar bolus would produce acoustic changes measurable by BARDS and that these would provide data on yeast metabolism.

In this study, BARDS is used for the first time together with HPLC to track the uptake of sugars by yeast and their metabolism to produce CO_2. These investigations were carried out using different strains of yeast and different carbon sources including monosaccharides (glucose and fructose) and disaccharides (maltose and sucrose).

The background to the principles of BARDS have been described by Fitzpatrick et al. (2012) and Crawford (1982). A brief outline of them are as follows.

The sound velocity (v) in a medium, whether air or liquid, is determined by Eq. (5)

$$V_{(sound)} = \sqrt{\frac{1}{K.\rho}} \quad (5)$$

where, ρ is mass density and *K* is compressibility which is the inverse of bulk modulus of the medium. The production of gas in a liquid decreases the density insignificantly compared to a significant increase in compressibility. This results in a significant reduction in the sound velocity in the system. The relationship between the fractional bubble volume and the sound velocity in water was derived by Crawford (1982), as given in Eq. (6).

$$\frac{v_{PBS}}{v} = \sqrt{1 + 1.618 \times 10^4 f_a} \quad (6)$$

Where v_{PBS} and v are velocities of sound in pure and bubble filled PBS respectively, and f_a is the fractional volume occupied by air bubbles. The constant 1.618×10^4 in the formula was calculated as shown in Eq. (7).

$$(v_{PBS})^2 \rho_{PBS} \frac{1}{\gamma p} = 1.618 \times 10^4 \quad (7)$$

where, ρ_{PBS} is the density of PBS, γ is the ratio of specific heats for CO_2 and p is the atmospheric pressure. Eq. (6) is based on the approximation presented originally by A.B. Wood (1930)

The BARDS technique is based on the induction of acoustic resonances in a liquid filled vessel, using a magnetic follower tapping against the inside vessel wall. The analysis is focused on fundamental resonance mode of the liquid. The frequency of this mode is determined by the sound velocity in the liquid and the approximate but fixed height of the liquid level, which corresponds to one quarter of its wavelength. The frequency response is described by Eq. (8).

$$freq = \frac{freq_{PBS}}{\sqrt{1 + 1.618 \times 10^4 f_a}} \quad (8)$$

where, *freq* and $freq_{IPBS}$ are the fundamental resonance frequencies in IPBS and in bubble filled IPBS, respectively.

2. Materials

Ale yeast (*Saccharomyces cerevisiae*) Nottingham Danstar lot no. 10863670367711X and Wheat Beer Yeast (*Saccharomyces cerevisiae*) Munich lot no. 10815380270611 V were purchased from Lallemand, UK. The bayanus yeast (*Saccharomyces bayanus*) was obtained from Bulldog brown lot no. 05229BJ. Active Dry yeast (*Saccharomyces cerevisiae*) lot no. 139007 was kindly received from Alltech, Sarney, Dunboyne, County Meath (Ireland). The following materials used were of analytical grade and purchased from Sigma–Aldrich, Glucose lot no. 129K0051, Fructose lot no. SLBQ0969 V, Maltose monohydrate lot no. SLBQ2371 V, and Sucrose lot no. 57-50-1.

3. Modelling

The extraction of rates for CO_2 production from the CO_2 gas volume graphs was performed using an approach as previously described (Vos et al., 2016; Ahmed et al., 2018).

4. Instrumentation

A BARDS spectrometer was procured from BASL Ltd. (BARDS Acoustic Science Labs, Cork, Ireland). A typical BARDS spectrometer consists of a chamber with a custom glass vessel, microphone and a magnetic stirrer and follower. The dissolution chamber can be accessed from the front and at the top in order to change the vessel or solvent and to place a sample in a weighing boat on a tipper motor for introduction of the solute. The microphone is positioned directly above the dissolution vessel within the housing. The resonances of the liquid vessel are monitored in a frequency band of 0–20 kHz. The microphone registers the acoustic resonance signals of the vessel which are converted in real time to a resonance frequency response using dedicated integrated computer software on a PC. Fig. 1 shows the instrument with external and internal views. A webinar showing the instrument in operation can be viewed at the following link: https://cams-uk.co.uk/webinars.

5. Experimental procedure

5.1. BARDS analysis

Phosphate-buffered saline (PBS, 25 mL at pH 7.4) was added into the BARDS glass vessel and equilibrated to 32 °C using a water bath. Once equilibrated to 32 °C, 0.5 g of yeast powder was added to the PBS solution and mixed well and conditioned at 32 °C for a further 10 min. The vessel was then placed in the BARDS instrument and glucose, or other sugar, was added from a weighing boat manually once the steady state frequency was reached. The liquid level is constant throughout all experiments and does not change upon addition of the yeast or the carbon source. The frequency time course of the fundamental resonance is presented, as manually extracted data from the resulting spectra. The steady-state frequency before addition of the powder is designated as the 'steady state'. It varies depending on the liquid volume in the vessel. Spectra were recorded for 3000 s depending on the rate of return of the

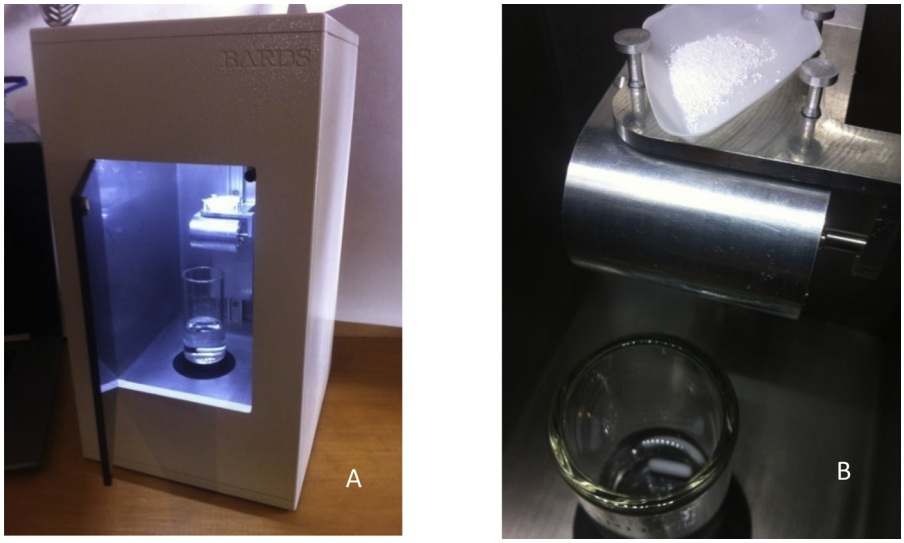

Fig. 1. (A) External view of the BARDS instrument and (B) Tipper motor with a sample of glucose in a weighing boat ready for addition to the stirring solution below, e.g. yeast suspension.

BARDS response to steady state. All experiments were performed in duplicate. However, triplicate experimental data is represented by the blue profile in Fig. 8 indicating significant reproducibility.

The temperature of the yeast suspension gradually decreased from 32 °C to room temperature after ~ 20 min. The speed of sound in IPBS at 35 °C is 1535 m s^{-1}. The speed of sound in IPBS at 30 °C is ~1525 m/s and at 25 °C it is 1512. Therefore, a drop from 32 to 25 °C (1525/1512 = 1.0) has an effect of a 1 % decrease, and a drop from 32 to 20 °C a ~2 % decrease on the freq $_{IPBS}$. The change in sound frequency as a result of temperature change can thus be considered negligible in the context of data interpretation for these experiments.

5.2. HPLC analysis

An Agilent 1260 HPLC instrument with a Refractive Index Detector (55 °C) was used. An Aminex HPX-87H (300 × 7.8 mm) column was used with an oven temperature of 60 °C. 5 mM H_2SO_4 was used as mobile phase with a flow rate of 0.6 ml/min. Injection volume was 20 µL. All the samples collected were filtered through 0.2 µm regenerated cellulose filters into 1.5 mL glass vials for analysis.

6. Results and discussion

In a typical BARDS experiment the background resonance frequencies of the vessel are recorded for 30 s, once stirring begins, before addition of the solute, which in this case is a carbon source for yeast. The solute is added, and the lag time before the dissolution signal is detected is seconds. In this case we hypothesized that the yeast would require time to take up the carbon source and metabolise it before carbon dioxide was released. We therefore anticipated that there would be an extended lag time before detection of a carbon dioxide signal. Once carbon dioxide is produced it changes the compressibility of the solvent which reduces the speed of sound in solution of the resonant frequencies which results in an audible pitch change. The frequency returns to the starting frequency after peak CO_2 production has been reached as the gas escapes at the surface. Deviations from a typical experiment will be highlighted in the following experiments.

6.1. Addition of Monosaccharide sugars to yeast suspensions

Fig. 2(A) shows the BARDS profiles for 0.5 g samples of ale yeast in 25 mL of IPBS solution with increasing concentration of glucose added at the 200 s time point. This time point was chosen because there is an initial drop in the frequency soon after the yeast suspension was placed in the BARDS instrument and stirred, due to entrained gas in the yeast suspension during reconditioning.

Glucose was added once the frequency was stabilised to a steady state, which took ~ 200 s. The addition of 40 mg of glucose to the yeast solution (at 200 s) shows an approximate lag-time of 650 − 700 s before an acoustic response is observed. This corresponds to the metabolic activation time taken by yeast cells to take up glucose, and produce the enzymes required for glucose metabolism before gaseous CO_2 is produced. The metabolism of glucose by yeast causes a significant decrease in the frequency showing a frequency minimum f_{min} of 6.7 kHz. This point was indicative of maximum CO_2 gas content of the yeast suspension during the experiment. The return slope is representative of an increased rate of CO_2 bubble loss from the solution compared to the rate of CO_2 production as a result of glucose metabolism. CO_2 gas gradually disappears from the solution by escape to the atmosphere at the surface allowing the spectra to return to steady state at 2500s. Increasing the glucose concentration from 40 to 60 mg results in a shorter lag-time with a reduction in f_{min} value to ~4.0 kHz and a faster return to steady state. The maximum loading of glucose (80 mg) showed a similar acoustic response time to that of 60 mg of glucose. However, a further decrease in the f_{min} to 3.75 kHz with a delayed return to steady state time (~2400s) was observed due to an increased amount of CO_2 production. The data demonstrate a shorter metabolic activation time and an increase in the metabolic rate of yeast with increasing concentration of glucose from 40 mg to 60 mg. A further increase in concentration to 80 mg did not increase the uptake rate above that of the 60 mg concentration. BARDS data is highly reproducible and the average standard deviation across spectral data points of triplicate measurements is 0.122 kHz. This allows for a reduction in replication to duplicate measurements with an average % variance of just 2.06 % for the data in this current paper. However, as this study deals with living cells, triplicate data is provided in Fig. 8 to add confidence to the overall data set.

The Crawford-Woods equation (Eq. 8) can be used to convert the frequency data observed in Fig. 2(A) to quantitative gas volume measurements. Fig. 2(B) displays the gas volume calculation for ale yeast solution with varying glucose additions. The data show the carbon dioxide gas content in solution due to metabolism of glucose by yeast during the experiment. The peak CO_2 content appears to be related to the concentration of glucose added. The up and down slopes indicate the rate of CO_2 gas production and loss from solution, respectively. The peak value is approximately the same for 80 mg as that induced by

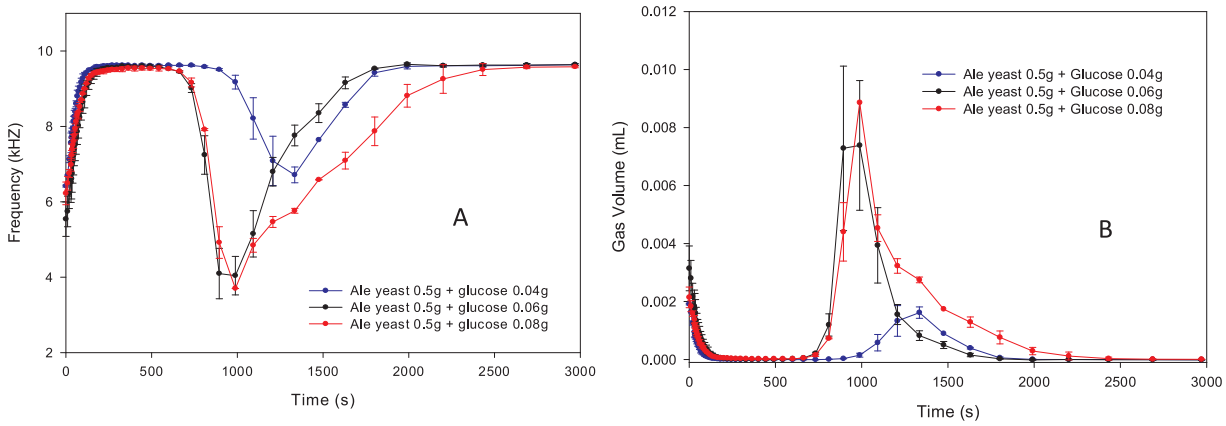

Fig. 2. (A) represents the BARDS profiles for 0.5g ale yeast dissolved in 25 mL of PBS solution with increasing concentration of glucose added at 200 s. Each profile is an average spread of duplicate experiments. (B) shows the gas volume data for the profiles in 2(A).

60 mg. However, more CO_2 is produced as indicated by the longer time to return to baseline. This result may indicate a concentration dependent uptake rate for glucose which is subject to a maximal limit. However, further studies will be required to confirm this hypothesis.

The next step was to apply the same assay to different strains of fermenting yeasts and to assess the effect of different sugars. Fig. 3(A) represents the BARDS profiles for metabolism of glucose by different fermenting yeasts in real time.

Wheat beer yeast strains do not produce any BARDS spectra upon the addition of glucose indicating a lack of gaseous CO_2 production.

The ale yeast solution when supplied with 80 mg of glucose showed a lag-time of 500 s as seen in the previous experiment. The spectra obtained demonstrate an f_{min} of ~ 3.6 kHz with a return to steady state time of 2500s. The profile for bayanus strain shows a longer lag-time of ~800 s followed by a f_{min} to 2.8 kHz and returns to steady state around 2500s. The spectra for active dry yeast displays the longest metabolic activation time with frequency decreasing to 6.7 kHz, which is followed by a rapid return to initial frequency value. The tracking of glucose metabolism of different strains of yeast by using BARDS demonstrates differences in their metabolic activation times and metabolic rates under standardised experimental conditions. Further work is required to determine if intrinsic strain-dependent differences in glucose uptake rates is a factor.

The data in the Fig. 3(A) were converted to gas volume and presented in Fig. 3(B). The wheat beer yeast does not show any CO_2 production or metabolism during a run time of 3000 s, therefore, the data show no response. Ale yeast dosed with glucose produces peak levels of 0.9×10^{-2} mL of CO_2 gas. Active dry yeast yields smaller amounts of CO_2 (1.8×10^{-3} mL) as a result of 80 mg of glucose provision. *S. bayanus* yields the maximum peak volume of CO_2 (1.57×10^{-2} mL) in comparison to the other yeasts tested.

Fig. 3(C) shows the BARDS spectra for the same yeast strains but with the addition of fructose as the carbon source instead of glucose. None of the four yeast suspension produced a BARDS spectrum. Although glucose and fructose are both hexoses it is known that *S. cerevisiae* is much slower to ferment fructose. This process takes a longer timeframe, therefore, no spectra were recorded in the default run time of 3000 s. Previous studies carried out by d'Amore (1989) and Guillaume (2007) also suggests that yeast uptake of glucose is faster than fructose.

In Fig. 4, glucose was added sequentially to the yeast suspension after the spectrum returned to steady state. The procedure was similar to the previous experiments with the exception that after the first addition of glucose the solution was stirred, during the lag-time, on a stirrer plate for 400 s.

The vessel containing the yeast suspension was then placed in the BARDS instrument and spectra were collected. This step effectively allowed the capture of 3600 s of data instead of 3000 s using the BARDS software. After the first addition of glucose, a total lag-time of 720 s was recorded after which gaseous CO_2 production is initiated and the frequency changes to $f_{min} = 7.2$ kHz, this represents the first acoustic response. The system was allowed to reach steady state and the second dose of glucose (80 mg) was added. The profile shows no lag-time, compared to the first addition of glucose, leading to instant detection of CO_2 production. Similar behaviour was observed for the subsequent additions of glucose. This suggests that the initial lag-time, also seen in Figs. 2(A), 3 (A) and (B) and 4, is a function of induction of transporters and enzymes for glucose metabolism, (Ozcan and Johnston, 1995; Boles

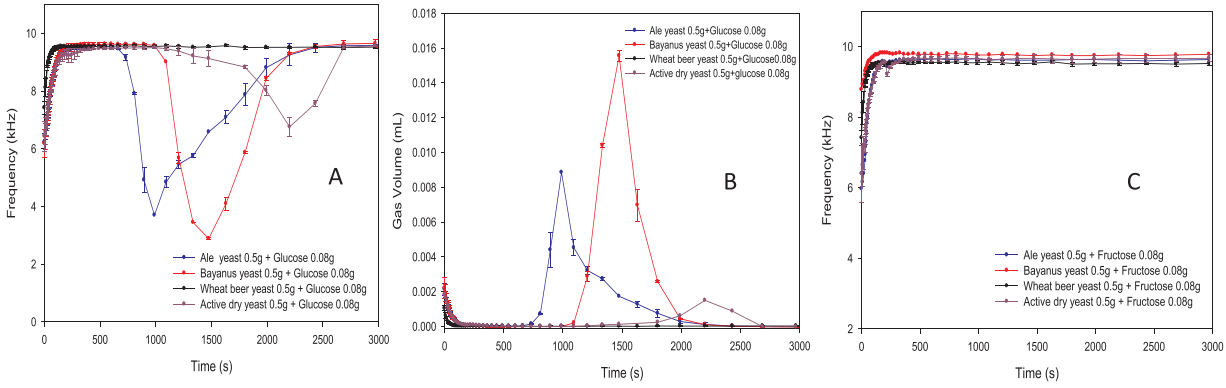

Fig. 3. (A) represents the BARDS profiles for metabolism of 80 mg of glucose by 0.5 g powder of different yeasts suspended in 25 mL of PBS solution. (B) Shows the gas volume plots for the data in Fig. 3(A). (C) BARDS data as a result of switching carbon source from glucose to fructose. Each profile is an average spread of duplicate experiments.

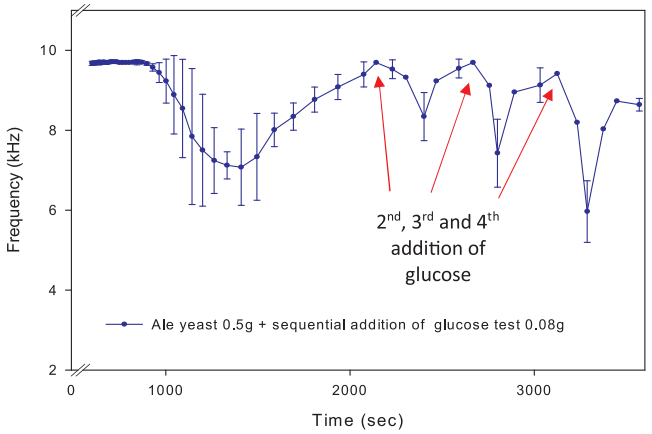

Fig. 4. (A) BARDS spectra for sequential addition of 80 mg of glucose to 0.5 g ale yeast dissolved in 25 mL of PBS solution. Note the break in the x-axis from 50 − 550 s Therefore the first addition of glucose is not shown at 200 s.

et al., 1993), The subsequent addition of glucose shows no lag-time as the transporters and enzymes required for metabolism are already present. This facilitates a rapid response by the yeast to the second and subsequent dosing leading to almost instantaneous CO_2 production

6.2. Di-saccharide sugars

Yeast metabolic studies were further continued by changing the carbon source from monosaccharides to disaccharides (maltose and sucrose) to study their impact on yeast metabolism. Fig. 5(A) displays the BARDS profiles for the addition of maltose to different yeast strains.

The data show that no change in the spectra was observed post-addition of maltose to the different yeasts during a run time of 3000 s. Maltose uptake by yeast requires expression of α-glucoside transporters and utilisation requires maltose expression before it enters the glycolytic pathway (Hatanaka et al., 2018). This can take up to 24 h before the metabolism process is initiated leading to CO_2 production (D'Amore et al., 1989).

Fig. 5(B) represents the BARDS responses for the metabolism of sucrose by the yeast strains in this study under the same experimental conditions. The profile for ale yeast upon addition of sucrose shows a lag-time of ~ 500 s before the onset of gaseous CO_2 production is detected. The spectrum obtained decreases to a f_{min} value of 5.7 kHz. The frequency gradually returns to steady state after 2200s. *S. bayanus* takes 50 s longer for CO_2 production to be detected. The profile shows a greater deflection to f_{min} with a faster return to steady state in comparison to ale yeast. However, both strains show a similar response to the addition of sucrose. Unlike maltose, in addition to cytoplasmic digestion (Marques et al., 2017), sucrose is readily hydrolysed into glucose and fructose by a periplasmic enzyme invertase and there are multiple hexose transporters for facilitated diffusion of glucose and fructose across the cell membrane. Given the lack of response to fructose shown in Fig. 3(C) for both yeasts, the BARDS signal is hypothesized to arise from glucose metabolism alone due to the breakdown of sucrose.

The data in Figs. 2, 3(A + B), (B) are consistent with the Crabtree Effect. This is the occurrence of anaerobic alcoholic fermentation in response to provision of a pulse of excess sugar to sugar-limited yeast cultures. This effect is reported to take place at glucose concentrations > 0.32 %. 40 mg of glucose in 25 mL = 0.16 %, and 80 mg in 25 mL = 0.32 %. However, a response for 40 mg of glucose addition is observed in Fig. 2(A). demonstrating a Crabtree Effect with a smaller mass of glucose.

Cross-Validation of BARDS data and HPLC data to track, glucose consumption, ethanol and CO_2 production.

BARDS measurements pre and post-addition of carbon source were compared with metabolite quantitation by HPLC analysis. The following data were obtained by conditioning 500 mg of *S. cerevisiae* at 32 °C in 25 mL of PBS solution. The yeast cell count was 1.44×10^{10} cells/g. The solution was transferred to a BARDS spectrometer after 10 min and data acquisition was commenced. 80 mg of glucose was added after 200 s to yield a 0.32 % solution. 1 mL samples were taken from the solution at six defined time points for HPLC analysis. The solution was supplemented with 1 mL of an 80 mg glucose 25 mL PBS solution after each sampling. Also, the glucose and ethanol concentrations require minor adjustment to account for their dilution during sampling. The resulting data are shown in Fig. 6(A).

The 25th-75th percentile volume range of yeast cells is ≈ $30 - 60 \times 10^{-12}$ mL. The median haploid volume of one yeast cell is 42×10^{-12} mL ± $2\ 10^{-12}$ mL. 500 mg of *S. cerevisiae* yeast in 25 mL of PBS solution was used in the experiment, therefore, there were 0.72×10^{10} cells in the solution. The resulting data in Fig. 6(B) shows a maximum CO_2 gas volume (Vol_{max}) of 3.48×10^{-3} mL. The estimated CO_2 gas elimination constant (k_{el}) is 3.6×10^{-2} s^{-1}. The maximum CO_2 gas generation rate = K_{el} x Vol_{max} = 1.25×10^{-4} mL s^{-1}. The CO_2 gas production rate per cell is ~ 1.25×10^{-4} mL s^{-1} /(0.72×10^{10}) = 1.74×10^{-14} mL s^{-1} of CO_2 per cell.

The data in Fig. 6(A) show that the glucose concentration begins to decrease immediately upon addition at 200 s. Ethanol production also begins to increase almost in unison with glucose consumption. Once the glucose concentration has dropped by 33 %, the gaseous CO_2 production commences, at first gradually and then rapidly. The rate of glucose

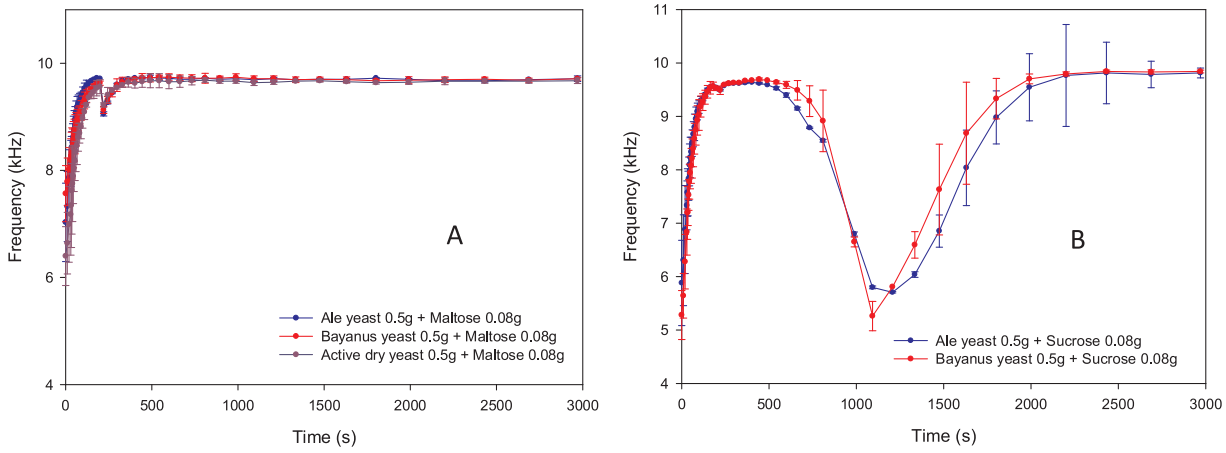

Fig. 5. (A) BARDS profiles for the addition of maltose (80 mg) to 500 mg of different yeast strains suspended in 25 mL of PBS. (B) The carbon source is changed to sucrose (80 mg). Each profile is an average spread of duplicate experiments. Note supplies of active dry yeast were not available for the sucrose experiments.

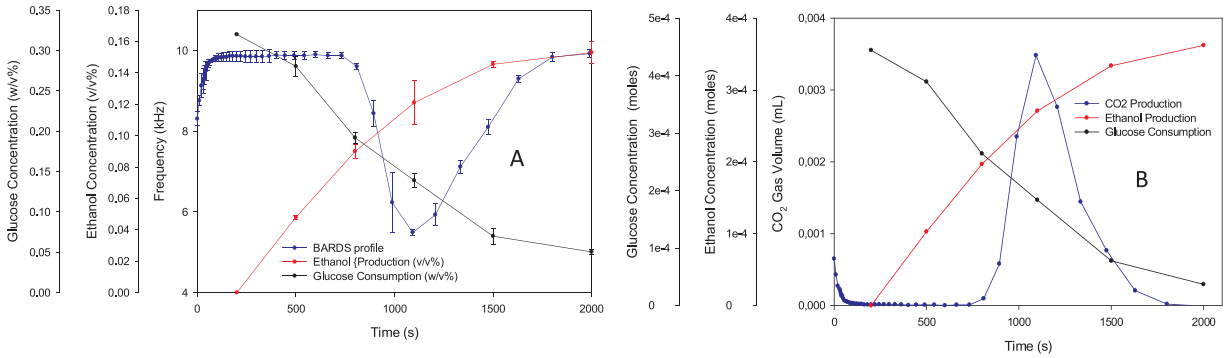

Fig. 6. (A) Comparison of the CO_2 BARDS profile with the glucose and ethanol concentration profiles, the latter two being measured by HPLC. (B) Comparison of gaseous CO_2 volume profile with glucose consumption and ethanol production profiles to illustrate the Crabtree Effect. The fractional gas volume data was derived from the frequency data in 6(A) using Crawford's equation.

consumption and ethanol production appear to be roughly similar. The BARDS frequency data were transformed using the Crawford equation (Eq. 8) to produce gas volume data for CO_2 gas production. The data are presented in Fig. 6(B).

Note not all CO_2 theoretically produced is detected in the gaseous form and further calculations are necessary to determine the ratio of gaseous/total produced CO_2 ratio (See section: *Quantitative analysis of CO_2 gas volume data presented in* Figs. 2, 3 and 4).

All the data were found to be reproducible for the duplicate measurements. There is one large error bar reading for gas volume before 1000s which may be attributable to the significant, rapid and erratic CO_2 production at this time point.

6.3. Sequential addition of carbon sources

The next part of the study involved evaluation of the effect of repeated boluses of sucrose. Fig. 7(A) shows BARDS data and production of ethanol post addition of sucrose at 200 s and 1800s.

Sucrose concentration reduction was tracked using HPLC with a downward trend observed. The BARDS spectra remains unchanged until 800 s but an increasing amount of ethanol is detected after 500 s. The frequency begins to decrease after 800 s and reaches f_{min} = 6.0 KHz thereafter, close to the ethanol maximum concentration post first sucrose addition. The profiles for ethanol production remains on a plateau until the second dose of sucrose was added at 1800s. The subsequent dose of sucrose results in no observable lag-time as seen with repeated glucose boluses (Fig. 4). Note the detection of CO_2 gas in relation to ethanol production is delayed when using sucrose compared to the same system where glucose was added. Fig. 7(B) shows ~80 % ethanol production correlating with 50 % gaseous CO_2 production.

The frequency changes observed during the metabolism of sucrose by yeast were now converted to gas volume data and presented in the Fig. 7(B). Peak CO_2 level and peak ethanol almost coincide. Sucrose concentration decreases from 0.32 % w/v to 0.04 ± 0.015 % w/v after 3000 s. The majority of the sucrose (80 %) is taken up in the first 300 s.

BARDS data for maltose metabolism by yeast cells showed negative results for the Crabtree response in Fig. 5(A). However, HPLC results indicated a modest increase in the amount of ethanol produced (0.08 % v/v) which was attained by ~ 1800s. CO_2 production remains below the threshold detectable by BARDS or is present in dissolved form. Theoretically, certain maltose strains should be metabolised by yeast as efficiently as sucrose but this was not observed during the BARDS experiments. This could be attributed to the type of yeast strain used in the study. Baking yeast was used which is cultured to metabolise glucose and sucrose more effectively, conversely, brewing yeast efficiently metabolises maltose.

6.4. Effect of temperature on yeast metabolism

The experimental method used involves a gradual decrease in temperature from 32 °C during the conditioning of the yeast to room temperature following its placement in the BARDS spectrometer. A control experiment, where the yeast was conditioned at room temperature was performed to investigate if there is an effect associated with this temperature decrease of approximately 10 °C. A delay of 140 s in the time taken to reach f_{min} was noted, however, the magnitude of f_{min} was unaffected as shown in Fig. 8.

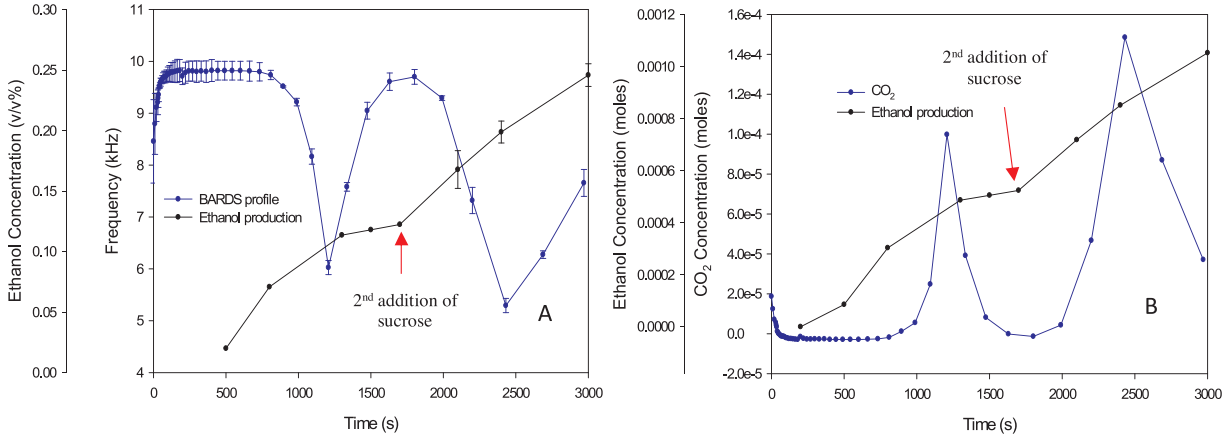

Fig. 7. (A) The comparison of the BARDS profile with ethanol production during the metabolism of sucrose (double dose) by Saccharomyces cerevisiae. (B) Gas volume data for the amount of CO_2 and ethanol production following the addition of 80 mg sucrose at 200 s and 1800s.

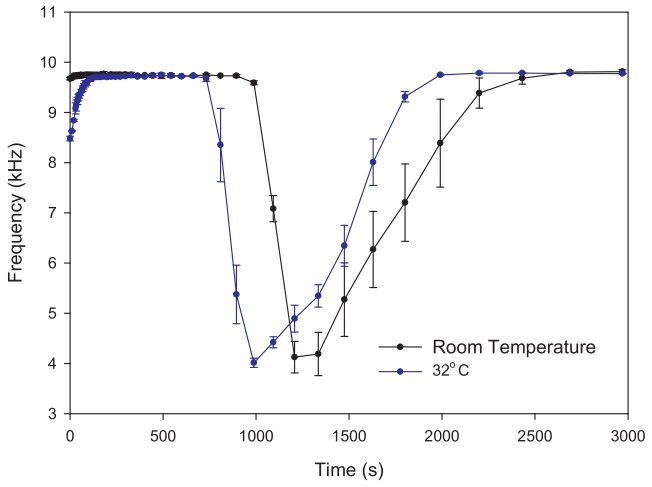

Fig. 8. The effect of temperature (STP) and 32 ºC on the BARDS response for Saccharomyces cerevisiae.

6.5. Mix-match experiments

An experiment was devised to determine the effect of switching the carbon source during a sequential addition experiment, i.e. whether an immediate response to dosing is present or not. It has been shown in Figs. 4 and 7 (A) that yeast will produce CO_2 immediately upon the second addition of glucose or sucrose. Fig. 9 (red profile) shows there is a 300 s delay in CO_2 production after the addition of sucrose following an initial dosing of glucose. However, the black profile shows there is no delay in CO_2 production upon repeat dosing of glucose. This sucrose lag-time (red profile 1800–2100 s) is approximately a third of the initial lag period (200–1000 s) and is presumably related to sucrose conversion to glucose.

Overall, the preceding experiments illustrate how BARDS analysis can be used to track yeast metabolism due to the Crabtree effect under a range of conditions with good reproducibility. There are many approaches to either inhibit or promote yeast metabolism through stressors or promoters such as resveratrol. BARDS analysis is therefore a unique and rapid test to measure the effect of such studies on yeast and possibly bacteria also. It may also be useful to check incoming consignments of yeast for vitality in a busy microbiology lab.

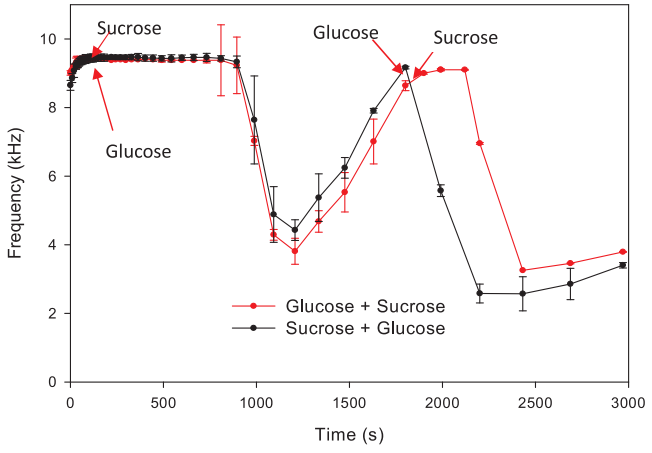

Fig. 9. Mix and match experiment where glucose was added at 200 s followed by sucrose at 1800 s (Red profile). The black profile represents the addition of sucrose at 200 s followed by the addition of glucose at 1800. (For interpretation of the references to colour in this figure legend, the reader is referred to the web version of this article).

7. Quantitative analysis of CO2 gas volume data presented in Figs. 2, 3(A + B), (B) and 6

The following data treatment helps to further elucidate the CO_2 gas volume time-courses obtained from the BARDS frequency data.

7.1. Rate constants for the first-order CO_2 gas elimination and disappearance processes

The rate constants for the disappearance of the entrained gases in the yeast suspensions during reconditioning (the volume curve data in the range of 30–180 s, Fig. 2(B)) were calculated to be 0.0206 - 0.0262 s^{-1} (Table 1).

In the calculations these values were taken as the first-order rate constants of the CO_2 gas elimination process (k_{el}). The rate constants are close to the previously obtained value for KCl dissolution in water (0.0286 s^{-1}).

A first order kinetic model for the conversion of glucose into CO_2 was not found to be representative of the observed kinetics shown in Figs. 2–8 but this is unsurprising given that it is a multistep process. More insight of the observed kinetics was obtained by determining the terminal CO_2 gas disappearance rate constant (assuming first order kinetics). The value of this disappearance rate constant ($k_{disappear}$) (Table 1) is an order of magnitude less than the value of the earlier mentioned gas elimination rate constant (k_{el}), indicating a flip-flop kinetic approach is required, at least after the attainment of the volume maximum, but most likely also before the volume maximum. The disappearance rate constant ($k_{disappear}$) can be considered as the rate constant for the gas generation process ($k_{generation}$). Thereby it should be noted that $k_{generation}$ is not representing a constant value, but a value increasing from zero (0) during the lag phase to a finite value (e.g., the earlier determined value $k_{disappear}$),(Vos et al., 2016).

7.2. Rates for the production of CO_2

It is not straightforward to derive rates for the production of CO_2 However, it is possible to estimate the CO_2 gas volume production rate from the maximum value of the CO_2 gas in the gas volume time course and gas elimination rate constant (k_{el}) for the suspension. This was reported for Fig. 6(A) above. At the maximum volume, the gas volume production rate ($\frac{d(\mathrm{Vol\ CO_{2(generation)}})}{\mathrm{dt}}$) equals the gas elimination rate ($\frac{d(\mathrm{Vol\ CO_{2(elimination)}})}{\mathrm{dt}}$), i.e., the CO_2 gas volume production rate is d(Vol CO_2 (production))/dt. (Note: generation means the same as production). The CO_2 gas volume elimination rate is given by Equation 11;

$$\frac{d(\mathrm{Vol\ CO_{2(elimination)}})}{\mathrm{dt}} = k_{el}.\ \mathrm{vol\ CO_2} \tag{11}$$

Whereby, Vol_{CO2} is the actual CO_2 volume at the maximum of the volume time course. A modelling approach was used to investigate the effect of concentration on the gas generation and elimination rates. The data in Fig. 2(B) were used to obtain the log plot in Fig. 10(A).

The gas generation and elimination rate constants were subsequently calculated from the slopes of these curves and are tabulated in Table 1.

The data in Table 1 show that initially the higher the glucose concentration the faster the gaseous CO_2 generation rate. However, a minor increase in the gas generation rate constant occurs above 60 mg of added glucose.

c. Experimental and theoretical CO_2 gas yields

Table 1 also includes the gas yield based on the experimental data and compared to the theoretical gas yield maximally expected from the addition of carbon source (sucrose) to *S. bayanus* assuming aerobic fermentation of only glucose and not fructose (see Equation 4). The experimental gas yields (EGY) are calculated from first-order rate constants of the CO_2 gas elimination process (k_{el}) and the area under the

Table 1
Calculated rate constants and gas yields for the addition of sucrose and glucose to 500 mg suspensions of various yeast strains, assuming aerobic fermentation.. (Note the kel value for KCl is 2.86×10^{-2} s^{-1}).

Expt. Parameter	Ale Yeast 80 mg Sucrose	Bayanus Yeast 80 mg Sucrose	Ale Yeast 40 mg Glucose	Ale Yeast 60 mg Glucose	Ale Yeast 80 mg Glucose	Ale Yeast 80 mg Glucose Fig. 6	Bayanus 80 mg Glucose
k Elimination (s^{-1})	2.67×10^{-2}	2.78×10^{-2}	2.62×10^{-2}	2.20×10^{-2}	2.06×10^{-2}	3.60×10^{-2}	2.24×10^{-2}
k Disappearance (s^{-1})	6.04×10^{-3}	6.28×10^{-3}	6.74×10^{-3}	6.24×10^{-3}	3.29×10^{-3}	–	6.76×10^{-3}
AUV (mL s)	1.84	1.62	6.85×10^{-1}	2.30	3.33	1.36	5.84
Time Range for AUV	1756	1756	1769	1769	1769	–	1769
Theoretical Gas Yield (mL)	1.12×10^{1}	1.12×10^{1}	1.07×10^{1}	1.60×10^{1}	2.13×10^{1}	2.13×10^{1}	2.13×10^{1}
Expt. Gas Yield (AUV k_{el}) (mL)	4.90×10^{-2}	4.50×10^{-2}	1.79×10^{-2}	5.06×10^{-2}	6.86×10^{-2}	4.91×10^{-2}	1.31×10^{-1}
Expt / Theoretical Yield	4.36×10^{-3}	4.01×10^{-3}	1.68×10^{-3}	3.16×10^{-3}	3.22×10^{-3}	2.30×10^{-2}	6.13×10^{-3}
Volume $_{max}$ (mL)	2.89×10^{-3}	3.85×10^{-3}	1.64×10^{-3}	7.24×10^{-3}	8.95×10^{-3}	3.48×10^{-3}	1.57×10^{-2}
Average Generation Rate (mL s^{-1}) *	2.79×10^{-5}	2.56×10^{-5}	1.01×10^{-5}	2.86×10^{-5}	3.88×10^{-5}	–	7.39×10^{-5}
Max Generation Rate (mL s^{-1}) **	7.71×10^{-5}	1.07×10^{-4}	4.30×10^{-5}	1.59×10^{-4}	1.84×10^{-4}	1.25×10^{-4}	3.50×10^{-4}
Theoretical Volume Yield / g (mL g^{-1})	1.40×10^{2}	1.40×10^{2}	2.66×10^{2}	2.66×10^{2}	2.66×10^{2}	2.66×10^{2}	2.66×10^{2}

* (AUV k_{el} / time range) mL/s).
** (Vol max k_{el}) mL/s).

gas volume time course (AUV) according to Eq. 12.

$$EGY = AUV.\ k_{el}. \quad (12)$$

The ratio between experimental and theoretical yield (Expt / Theor) is O(10e-3), which is significantly lower than expected. However, similar observations with BARDS calculated CO_2 gas yields were previously reported by Ahmed et al. (2018) in respect of CO_2 produced during acid-base reactions.

The same approach was used again to investigate the gas generation and elimination kinetics for the metabolism of glucose to *S. bayanus*. Fig. 10(B) shows the gas volume log plot for the addition of 80 mg of glucose to 500 mg of *S. bayanus* in 25 mL of PBS. The raw data was obtained from Fig. 3(B). Table 1 shows the gas generation and elimination rate constants calculated from the slopes of Fig. 10(B). The elimination rate constant is slightly higher for the *S. bayanus* suspension. However, the gas generation rate is almost double that of *S. cerevisiae*.

Table 1 also shows calculated rate constants and gas yields for the addition of 80 mg sucrose to 500 mg of *S. bayanus* in 25 mL of PBS solution. The data has been generated from the data in Fig. 11(A) which has then been transposed into the log scale for Fig. 11(B) to obtain straight line slopes.

Fig. 11(C + E) show the regression plots of the gas volume responses after addition of *S. cerevisiae* and *S. bayanus*. These were used for estimation of the CO_2 gas elimination rate constants experiments. A volume maximum of 2.89×10^{-3} and 3.85×10^{-3} mL were obtained for *S. cerevisiae* and *S. bayanus* respectively. Fig. 11(D + F) show regression plots for the CO_2 disappearance rates post addition of sucrose to *S. cerevisiae* and *S. bayanus*. *S. cerevisiae* exhibits a slightly higher generation rate constant (2.79×10^{-5} mL s^{-1}) in comparison to *S. bayanus* (2.56×10^{-5} mL s^{-1}).

8. The relationship between glucose consumption and ethanol production (theoretical vs experimental)

Fig. 12 shows that the amount of ethanol has increased from 0 moles at 200 s to 7.24×10^{-4} moles at 2000s. The amount of glucose has decreased from 4.44×10^{-4} moles at 200 s to 3.68×10^{-5} moles at 2000s. The ratio of ethanol production vs glucose consumption = 1.78 (7.24×10^{-4} - 0)/ (4.44×10^{-4} - 3.68×10^{-5}) = 7.24×10^{-4} / 4.07×10^{-4} = 1.78). This ratio is only slightly lower than the theoretically expected value of 2.

9. Comparison of experimental CO_2 yield with theoretical yield

The profiles for glucose in Fig. 6 show that 91.7 % glucose has been

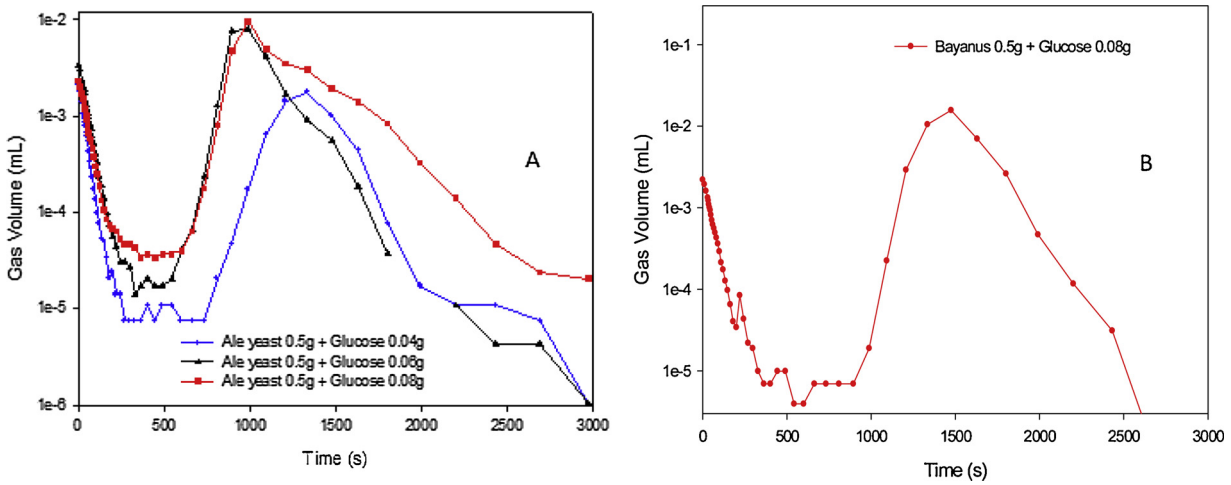

Fig. 10. (A) The gas volume log plots for the addition of a range of concentrations of glucose to 500 mg of Saccharomyces cerevisiae in 25 mL of PBS buffer. (B) The gas volume log plot for the addition of 80 mg of glucose to 500 mg of Saccharomyces bayanus. The raw data were obtained from Figs. 2 and 3(B).

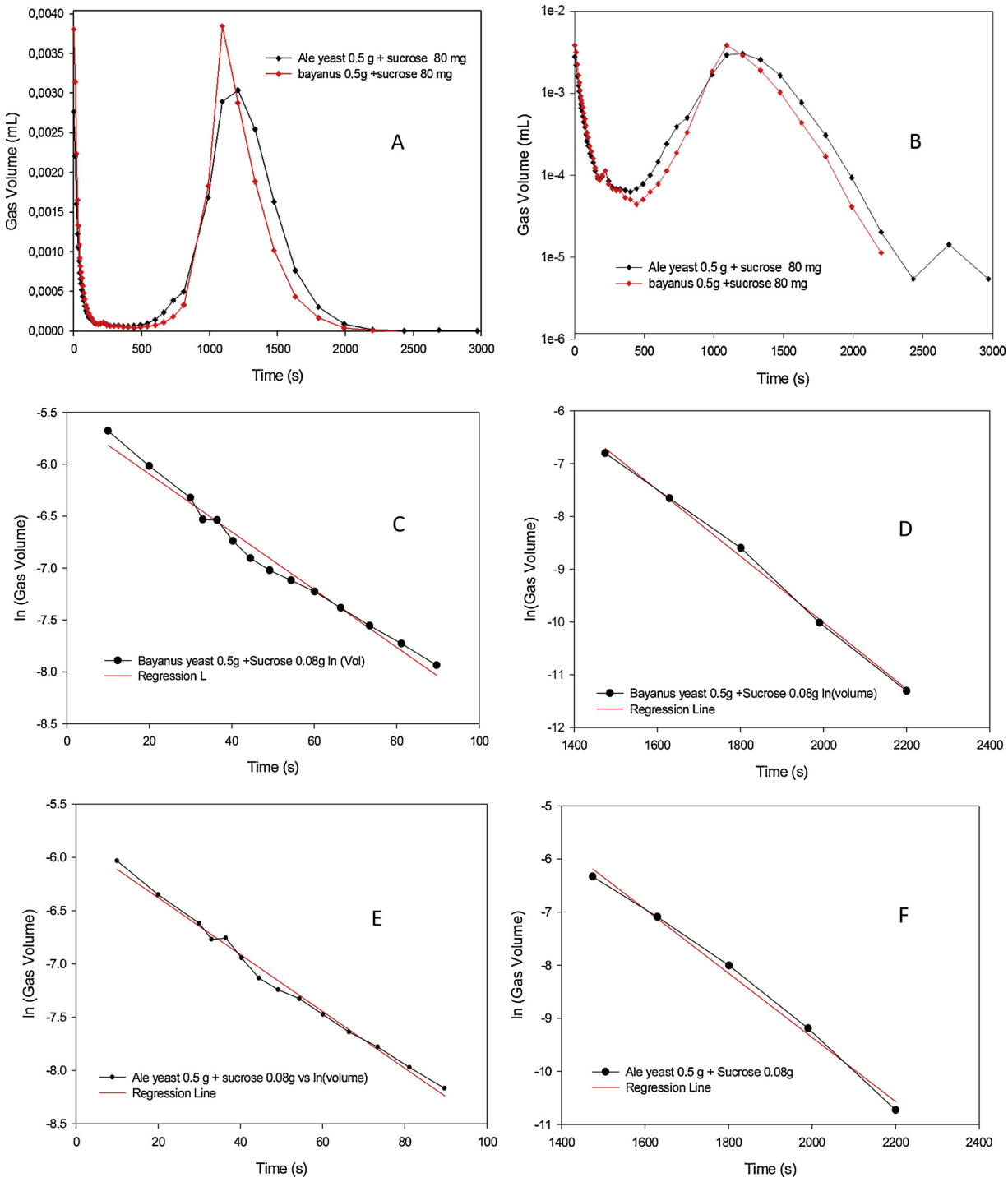

Fig. 11. (A) Gas volume plots for the addition of 80 mg sucrose to 500 mg Saccharomyces cerevisiae and Saccharomyces bayanus in 25 mL of PBS buffer. (B) The data in (A) transposed to a log scale. (C and E) Regression analysis for gas elimination rate (k_{el}) and (D and F) regression analysis for gas generation rate, both in the same systems as (A).

used by 2000s, (4.07×10^{-4} / 4.44×10^{-5} x 100 % = 91.7 %). An experimental gas yield of 4.91×10^{-2} mL was observed for the data in Fig. 6. A ratio of experimental / theoretical gas yield of 2.30×10^{-3} is observed using a theoretical gas yield for 80 mg glucose of 21.3 mL. However, using the actual amount of glucose used (80 × 0.917 mg) yields a theoretical value of 19.5 mL (21.3 × 0.917 = 19.5 mL). The ratio experimental/theoretical gas yield then becomes 2.52×10^{-3}.

Fig. 6 also shows that the production of ethanol is evident (200 s) soon after the addition of glucose. However, there is no frequency change associated with the evolution of carbon dioxide until 800 s. This may be due to a delay in CO_2 bubble formation or a lack of sensitivity of BARDS until a threshold level of gaseous CO_2 is reached. Liger-Belair (2004) has reported the rigidification of bubbles in the presence of a surrounding monolayer of surfactant around bubbles. This could reduce their compressibility and affect a BARDS signal. However, this is difficult to translate to the signal delay in the current study.

It should be also noted that ethanol can also have an effect on the speed of sound as outlined by Lara and Desnoyer (1981). However, the concentration of ethanol produced will have an insignificant effect in comparison to the evolution and presence of CO_2. If ethanol were

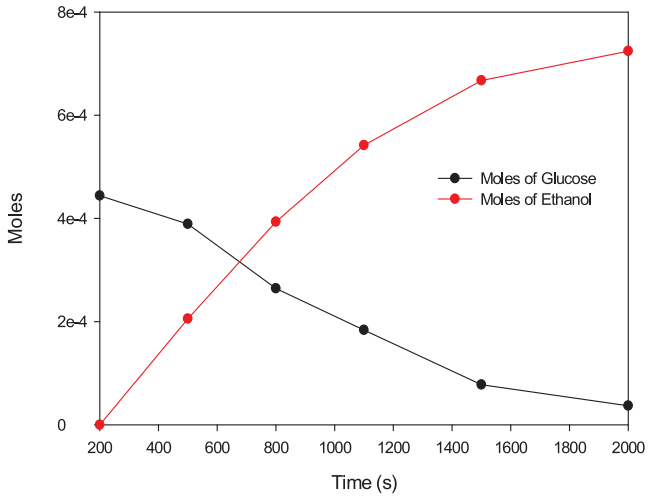

Fig. 12. The relationship between glucose consumption and ethanol production.

responsible for the changes in the speed of sound, then the frequency would change and correlate with the increase in ethanol as measured by HPLC. This is not the case. Also, if ethanol were responsible for frequency changes then the frequency would remain depressed as ethanol is not lost from solution. This is also not the case as the frequency recovers back to steady state. This behaviour can only be explained by CO_2 evolution and loss.

10. Conclusions

In this study, BARDS has proven effective as a reproducible method to investigate yeast metabolism for the strains investigated. BARDS data correlates with the kinetics of yeast sugar metabolism and the production of ethanol as established by simultaneous HPLC measurement. A defined strain-specific lag-time associated with the carbon source is evident and reproducible under the conditions used. The kinetic data also shows that the gaseous CO_2 production and elimination rates can be modelled. Consistent strain-specific values were obtained for maximum BARDS signal and BARDS-derived maximum CO_2 generation rates when using the same carbon sources. The volume of CO_2 detected as gas in the yeast suspensions, measured by applying the Crawford's equation to BARDS data, was consistently 1 % or less of the predicted volume of CO_2 evolved from sugar consumption and ethanol evolution. This means the vast majority of the CO_2 passing from yeast into culture media in the experimental conditions described is in solution with diffusion loss from the fluid surface. The delay in the start of the BARDS signal, after ethanol production is detectable, suggests that there is a threshold concentration of dissolved carbon dioxide required for bubble formation. The yeast cell surface would be the leading candidate for bubble nucleation in our system due to the lack of other sufaces. Measurable BARDS signals over the data gathering period of 50 min were obtained with glucose and sucrose, but not fructose or maltose, suggesting that glucose is the key substrate whose metabolism underlies the effect. The inhibition of BARDS-measured sucrose metabolism by glucose but not vice versa corresponds to the published hierarchy established using standard methodology. Currently, time consuming HPLC and flow cytometric methods are used to characterise vitality and attenuation of yeast strains for individual batches of yeast. The data presented shows that BARDS may have the potential to provide a rapid simple test for the early detection of the common phenomenon of an aberrant fermentation profile in recycled wort, which is generally attributed to mutations giving rise to a "petite" cell phenotype effect, (Gibson et al., 2008).

Author contribution

M.Rizwan Ahmed,

Dr. Ahmed carried out the majority of experiments as a post-graduate student working in Dr. Fitzpatrick's laboratory.

Nicholas Doyle

Carried out experiments using fructose as a M.Sc. minor thesis study.

Dr. Cathal Connolly

Associate Director of Research for Alltech Ltd who co-sponsored the postgrad studentship and contributed samples, interpretation and mentorship during the project.

Dr. Seán McSweeney

Is the engineer who developed the BARDS hardware and software as a postdoctoral researcher under Dr. Fitzpatrick.

Dr. Jacob Krüse

Provided all the modelling and predictions in the paper

Dr. John Morrissey

Specialist in yeast microbiology who provided yeast samples and made sure we were working on the correct lines of enquiry.

Prof. Michael B Prentice

Clinical microbiologist who conceived the initial experiments to track CO_2 due to yeast metabolism

Dr. Dara Fitzpatrick

Originator of BARDS and supervisor to Rizwan Ahmed during the studies. Secured funding and authored and edited the paper.

Declaration of Competing Interest

Drs. Sean McSweeney and Dara Fitzpatrick are directors of BARDS Acoustic Science Labs Ltd which is a spin out company from University College Cork Acknowledgements

Acknowledgements

This work was co-funded by Alltech (Ireland) Ltd. and the Irish Research Council (Ireland) who generously sponsored the studentship of Rizwan Ahmed under grant number IRC/EPSPG/2014/84.

We wish to state that Drs. Seán McSweeney and Dara Fitzpatrick are directors of BARDS Acoustic Science Labs Ltd.

References

Ahmed, M.R., McSweeney, Sean, Krüse, Jacob, Vos, Bastiaan, Fitzpatrick, Dara, 2018. Contactless, probeless and non-titrimetric determination of acid–base reactions using broadband acoustic resonance dissolution spectroscopy (BARDS). Analyst 143 (4), 956–962.

Boles, E., Zimmermann, F.K., Heinisch, J., 1993. Different signals control the activation of glycolysis in the yeast Saccharomyces cerevisiae. Yeast 9 (7), 761–770.

Crawford, F.S., 1982. The hot chocolate effect. Am. J. Phys. 50 (5), 398–403.

Fleet, G.H., 1998. Yeasts-What reactions and interactions really occur in natural habitats. Food Technol. Biotechnol. 36, 285–290.

Fitzpatrick, D., Krüse, Jacob, Vos, Bastiaan, Foley, Owen, Gleeson, Donncha, O'Gorman, Eadaoin, O'Keefe, Raymond, 2012. Principles and Applications of Broadband Acoustic Resonance Dissolution Spectroscopy (BARDS): A Sound Approach for the Analysis of Compounds. Anal. Chem. 84 (5), 2202–2210.

Gibson, B.R., Prescott, K.A., Smart, K.A., 2008. 'Petite mutation in aged and oxidatively stressed ale and lager brewing yeast. Lett. Appl. Microbiol. 46 (6), 636–642.

Goffeau, A., Barrell, B.G., Bussey, H., Davis, R.W., Dujon, B., Feldmann, H., Galibert, F., Hoheisel, J.D., Jacq, C., Johnston, M., Louis, E.J., Mewes, H.W., Murakami, Y., Philippsen, P., Tettelin, H., Oliver, S.G., 1996. Life with 6000 genes. Science 274 (5287), 546–567.

Guilliermond, A., 1920. The Yeasts. John Wiley and Sons Incorporated.

Harden, A., Young, W.J., 1906. The alcoholic ferment of yeast-juice. Proc. R. Soc. Lond. B 77 (519), 405–420.

Hatanaka, Haruyo, Mitsunaga, Hitoshi, Fukusaki, Eiichiro, 2018. Inhibition of S. Cerevisiae growth by simultaneous uptake of glucose and maltose. J. Biosci. Bioeng. 125 (1), 52–58.

Kresge, N., Simoni, R., Hill, R.L., 2005. Otto Fritz Meyerhof and the elucidation of the glycolytic pathway. J. Biol. Chem. 280 (4).

Lagunas, R., 1993. Sugar transport in S. cerevisiae. FEMS Microbiol. Lett. 104 (3-4), 229–242.

Lara, J., Desnoyerm, M., 1981. Isentropic compressibilities of alcohol-water mixtures at 25°C. J. Solution Chem. 10 (7), 465–478.
Liger-Belair, Gérard, 2004. Uncorked: The Science of Champagne. Princeton University Press.
Marques, W.L., Mans, R., Marella, E.R., Cordeiro, R.L., van den Broek, M., Daran, J.-M.G., Pronk, J.T., Gombert, A.K., van Maris, A.J.A., 2017. Elimination of sucrose transport and hydrolysis in S. cerevisiae: a platform strain for engineering sucrose metabolism. FEMS Yeast Res. 17 (1).
Nilsson, A., Nielsen, J., 2016. Metabolic trade-offs in yeast are caused by F1F0-ATP synthase. Sci. Rep. 6, 22264.
Oliver, S.G., van der Aart, Q.J., Agostoni-Carbone, M.L., Aigle, M., Alberghina, L., Alexandraki, D., Antoine, G., Anwar, R., Ballesta, J.P., Benit, P., 1992. The complete DNA sequence of yeast chromosome III. Nature 357 (6373), 38.
Ozcan, Sabire, Johnston, Mark, 1995. 'Three different regulatory mechanisms enable yeast hexose transporter (HXT) genes to be induced by different levels of glucose. Mol. Cell. Biol. 15 (3), 1564–1572.
Pfeiffer, T., Morley, A., 2014. An evolutionary perspective on the Crabtree effect. Front. Mol. Biosci. 1, 17.
Swart, Chantel W., Dithebe, Khumisho, Pohl, Carolina H., Swart, Hendrik C., Coetsee, Elizabeth, van Wyk, Pieter W.J., et al., 2012. 'Gas bubble formation in the cytoplasm of a fermenting yeast. FEMS Yeast Res. (7), 867–869.
Vos, B., Crowley, S.V., Evans-Hurson, R., McSweeney, S., Krüse, Fitzpatrick D., O'Mahony, J.A., 2016. New insights into the mechanism of rehydration of milk protein concentrate powders determined by Broadband Acoustic Resonance Dissolution Spectroscopy (BARDS). Food Hydrocoll. 61, 933–945.
White, J., 1954. Yeast Technology. Chapman and Hall Ltd, London.
Wood, A.B., 1930. A Textbook of Sound. Macmillan.